Research Article

Risk Area Identification Model of Bus Bay Stops Based on Distribution of Conflicts

Weiwei Qi [iD],[1] Lianjie Ruan [iD],[1] Yue Zhi [iD],[2] and Bin Shen [iD][3]

[1]*School of Civil Engineering and Transportation, South China University of Technology, Guangzhou 510641, China*
[2]*School of Rehabilitation Engineering, Binzhou Medical University, Yantai 264003, China*
[3]*Urban Planning Design Institute of Ganzhou, Ganzhou 341000, China*

Correspondence should be addressed to Yue Zhi; zhiyue@bzmc.edu.cn

Effective identification of the risk area of the bus bay stop is a prerequisite for the enhancement of traffic safety. This study proposes a method of identifying the risk area based on the distribution of traffic conflicts. Firstly, the traffic flow data of the bus stop is collected by drones and video recognition software, and the traffic flow characteristics of the bus stop are analyzed by the mathematical and statistical methods. Secondly, using the gray clustering evaluation theory, on the basis of the rasterization of the functional area of the bus bay stop, a risk level model based on the index system of conflict rate, conflict severity, and potential conflict risk is proposed. Finally, take a bus stop in Guangzhou as an example to verify the solution. The results show that the constructed model can effectively identify the risk areas of bus bay stops. The risk areas of the bus bay stops are concentrated in the middle and lower reaches of the bus stop, which proves that the impact of bus exiting the stop on the surrounding traffic is greater than the process of bus entering the stop; the traffic risk areas of lanes near the bus stop are concentrated, and the severity of conflicts is low. The traffic risk zone of the lane far away from the bus stop is widely distributed, and the severity of conflict is higher. The research results can provide a basis for the micro safety performance evaluation and safety optimization of bus bay stops, which has strong theoretical and practical significance.

1. Introduction

With the development of urbanization in China, the pressure of urban traffic is increasing gradually. In recent years, scholars have proposed many ways to try to solve this problem, such as efficient transportation systems [1], travel restrictions [2], and ridesharing service [3]. In the meantime, large-capacity and high-efficiency travel modes are gaining more and more attention. Public transportation priority has become an important way to solve urban transportation problems due to its large size, flexibility, low pollution, and low cost [4, 5]. A high-quality public transportation system will attract urban residents to use it, which furthermore helps to alleviate traffic congestion, reduce energy consumption, and reduce air pollution [6]. In order to improve the quality of bus services, scholars have carried out a lot of research on vehicle scheduling [7–9], public transportation

priority [10], demand prediction [11], and trip time prediction [7]. Given the growing demand, traffic safety is very important to everyone, and it also greatly affects traffic efficiency. Therefore, actions can be taken to identify safety hazards, thereby improving the whole transportation system.

The bus stop is an important part of the public transportation system, and its service level has a significant influence on the overall quality of the urban public transportation system [12]. In order to better meet the needs of residents and bus companies, bus stops are generally set up in shopping malls, residential communities, entertainment venues, and other places with heavy traffic, which often makes bus stops adversely affect traffic operations. According to its geometric shape, bus stops can be divided into bus bay stops and online bus stops. In the process of entering and exiting the bus bay stop, public transportation

vehicles will diverge, merge, or even interweave with the main line traffic flow. Especially during the peak period, when the traffic volume increases and the headway decreases, various conflicts occur during the bus entering and exiting the stop, which brings security risks to the entire transportation system. However, the design of bus stops is mostly independent of roads. For decades, few studies have examined the interactions between bus stops and roads. The lack of research on the interaction makes the traffic in the bus stop functional area chaotic and hinders the quality improvement of the transportation system.

There are many factors that affect the level of traffic safety, especially at bus stops. Several studies used regression analysis to quantify the frequency of bus crashes under different factors. Ye et al. used principal component analysis and k-means clustering methods to model and quantify safety levels for bus stops [13]. Chimba et al. assessed the impact of vehicle size on the frequency of accidents [14]. Amadori and Bonino calculated the safety level of the bus stop based on the combination of the probability of occurrence and the severity of the accident [15]. Cheranchery et al. proposed a fuzzy evaluation method for bus stops by identifying unsafe behaviors in and around bus stops and their causal factors [16]. Truong and Somenahalli selected and ranked bus stops in pedestrian-vehicle crash hot spots based on the severity of pedestrian-vehicle crashes in their vicinities [17].

Unfortunately, the number of accidents may not be a true indication of safety problems. Statistical time periods and other detailed traffic information make rapid risk analysis impossible. In order to overcome the limitations of accident data, relevant research on traffic conflict has been paid more and more attention. The essence of traffic conflict is a manifestation of unsafe traffic behavior, and it is a potential accident where drivers do not take measures. Many previous studies have found that there is a strong correlation between traffic conflicts and traffic accidents [18–25]. Compared to accident data analysis, traffic conflict analysis can be carried out within a relatively short period without observing traffic crashes for years. Traffic conflict analysis is first widely used in the safety assessment of intersections [26–29]. With the deepening of research, highway sections are gradually using traffic conflict technology for risk analysis, such as weaving area [30, 31].

Gray clustering analysis, as an important clustering technique, has been widely used in many fields such as safety evaluation of civil aircraft [32], hazard assessment of drought disaster [33], waterlogging hazard evaluation [34], and nautical navigational environment risk evaluation [35]. It can consider the influence of multiple factors of the evaluation indicators and accurately reflect the road traffic safety status through a small number of indexes. Therefore, the use of gray clustering theory for traffic safety evaluation is no exception. Zhou et al. studied the application of gray clustering in traffic accident analysis [36].

Hence, based on the theory of traffic conflicts, this study constructs a bus bay stop risk area identification model to realize the identification of traffic conflict risk areas and provide a reference for optimizing the safety level of the bus stop functional area.

The rest of this paper is organized as follows. Section 2 describes the method of data collection in detail. Section 3 analyzes the traffic flow characteristics of the stop from two aspects: speed distribution and lane-changing behavior. Section 4 reports the gray clustering and risk area identification model. Section 5 introduces a case based on a bus stop in Guangzhou and specific identification results. Finally, Section 6 presents the conclusions of this study and suggestions for future work.

2. Experiment Design

2.1. Video Collection. A bus bay stop in Guangzhou was selected as the research object of this experiment. The sample stop is located on the urban expressway, and there are eighteen bus lines running during evening peak hours. The platform length of the sample stop is 40 m, the transition section is 20 m, the harbor depth is 3.0 m, and the number of mainline lanes is 4, as shown in Figure 1.

tThe survey was conducted mainly by aerial photography with the Unmanned Aerial Vehicle (UAV [37]). The main experimental equipment in this article is the DJI "Mavic air 2" UAV platform, which clearly records the shooting scene with 4 k/60fps video. The field of view is 84°, which is sufficient to record the survey range of 50 meters upstream and downstream of the bus stop in this study. Combined with the actual situation, each time the UAV rises to a height of about 170 meters, the aerial video range covers the entire range of bus stop functional area required for the study. The survey is conducted from August 26, 2020, to August 28, 2020, during the peak hours of the weekday evening. The UAV took 15–20 minutes of aerial video each time and got about 150 minutes of original video data.

2.2. Traffic Conflict Collection. Since the concept of traffic conflict was introduced, there have been about 40 evaluation metrics used to measure traffic conflict after continuous research and exploration by scholars, such as time to collision (TTC) [38–40], postencroachment time (PET) [41], time advantage (TADV) [42], and noncomplete braking time (TB) [43]. For theoretical and reliability reasons, TTC is more commonly used in practice than many other evaluation metrics. Combined with the characteristics of traffic conflicts at bus bay stops, this study selects TTC as a measure of traffic conflicts.

The traffic conflict is divided into two types: rear-end conflict and lane-change conflict. The formula of TTC for rear-end conflict is shown in the following equation:

$$\text{TTC}_i(t) = \frac{x_{i-1}(t) - x_i(t) - L_{i-1}}{v_{x,i}(t) - v_{x,i-1}(t)}, \tag{1}$$

where x_i and $v_{x,i}$ represent the position and speed of the following vehicle, respectively; x_{i-1} and $v_{x,i-1}$ denote the position and speed of the preceding vehicle, respectively; and L_{i-1} is the length of the preceding vehicle. In practical application, the calculation principle of TTC is shown in equation (2) and Figure 2. During the whole process of one
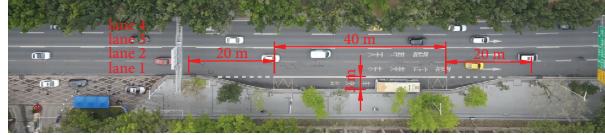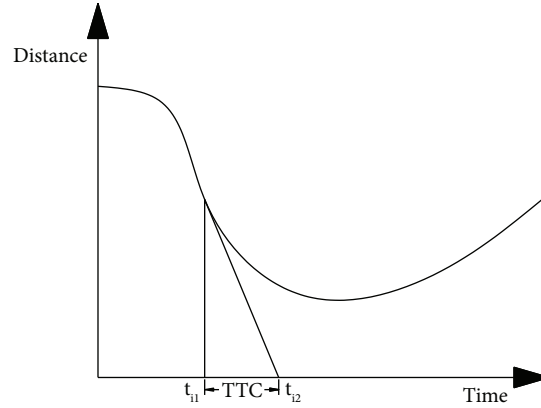
FIGURE 1: Sample stop of bus bay stop.

FIGURE 2: Schematic diagram of TTC calculation for rear-end conflict.

rear-end conflict, the smallest TTC_i in the relative distance-time curve of two vehicles is counted as the TTC value of this rear-end conflict.

$$TTC = t_{i2} - t_{i1}. \quad (2)$$

For the lane-change conflict, the speed of the two vehicles V_1 and V_2 in the traffic conflict, the length L_1 and L_2 of the two vehicles, and the distances S_1 and S_2 between the two vehicles from the conflict point are shown in Figure 3.

The calculation of TTC is divided into the following situations:

Case 1: $(S_1/V_1) = (S_2/V_2)$

This conflict is valid, $TTC_i = (S_1/V_1) = (S_2/V_2)$.

Case 2: $(S_1/V_1) > (S_2/V_2)$

If $S_1/V_1 < (S_2/V_2) + (L_2/V_2)$, then this conflict is valid and $TTC_i = (S_1/V_1)$; if $(S_1/V_1) \geq (S_2/V_2) + (L_2/V_2)$, then this conflict is invalid.

Case 3: $(S_1/V_1) < (S_2/V_2)$

If $(S_2/V_2) < (S_1/V_1) + (L_1/V_1)$, then this conflict is valid and $TTC_i = (S_2/V_2)$; if $(S_2/V_2) \geq (S_1/V_1) + (L_1/V_1)$, then this conflict is invalid.

This experiment mainly uses the software Tracker 4.95 for video data processing. According to the actual situation, a suitable Cartesian coordinate system and scale are established, and then the target vehicle can be tracked easily to get the trajectory data, speed data, and so on. By calibrating and tracking the vehicles with the software Tracker, the distance data of two vehicles can be easily obtained, as shown in Figures 4 and 5.

3. Characteristic of Traffic Flow

3.1. Speed Characterization. Based on the video data of the bus bay stop captured by the UAV, the video is processed by Tracker software to obtain sample data of vehicle speed in the functional area of the stop. In order to deeply explore the speed distribution characteristics, the speed samples were divided according to the driving lanes. The speed distribution of each lane is shown in Figure 6, and the lane speed characteristic values are shown in Table 1.

Overall, the speed of lane 1 near the bus stop is the lowest, and the dispersion of speed is larger; the speed of each lane decreases in the order of the inner lane to the outer lane, and the dispersion of speed increases in the order of the inner lane to the outer lane. According to analysis, the process of exiting the bus bay stop has serious interference with vehicles in adjacent lanes. In order to reduce this interference as much as possible, some vehicles will choose to change lanes, so the vehicles in the middle lane are also affected. Therefore, the speed and the speed dispersion of each lane are constantly changing, and finally the speed of the lane decreases from the outside to the inside, and the speed dispersion of the lane increases from the outside to the inside.

3.2. Analysis of Lane-Changing Behavior. Vehicle lane-changing behavior is an important cause of traffic conflicts, and exploring the vehicle lane-changing characteristics of the bus bay stop is the basis for studying the traffic conflict characteristics. According to the video of UAV, the location information of each vehicle generating lane-changing behavior in the functional area can be obtained with the help of the software Tracker. Based on the collected vehicle lane-
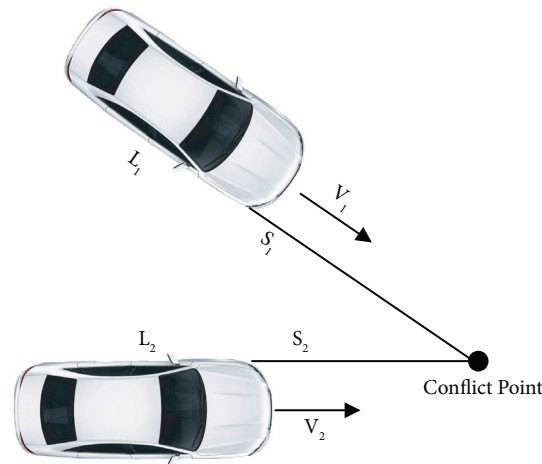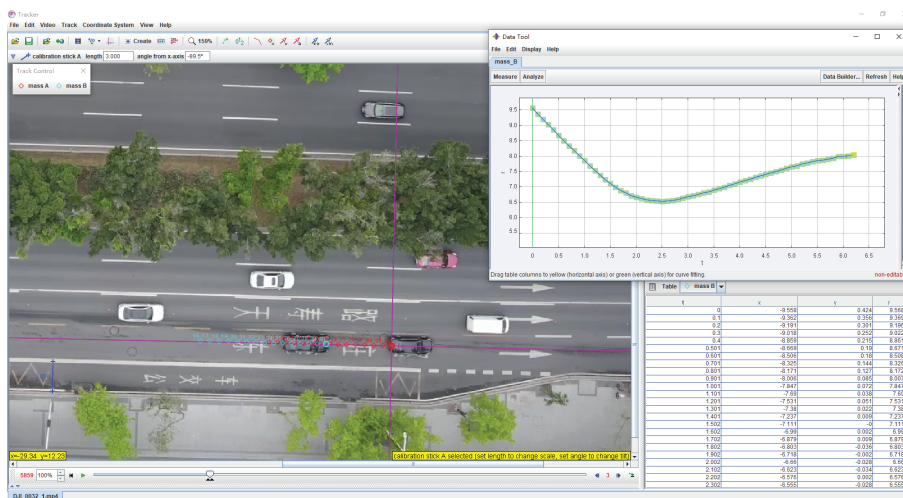
FIGURE 3: Lane-change conflict diagram.

FIGURE 4: Schematic diagram of extracting rear-end conflicts.

changing data, draw a heat map of vehicle lane-changing point distribution, as shown in Figure 7.

As the heat map shows, there are the most lane-changing vehicles on lane 2, and the lane-changing behavior runs through the entire functional area. The number of lane-changing vehicles on lane 1 is second only to lane 2, and the lane-changing points are mainly concentrated in the upper and middle areas of the functional area. Lane 3 has fewer lane-changing vehicles, and the distribution of lane-changing points is more scattered. Lane 4 is the innermost lane, and the number of lane-changing vehicles is the smallest.

4. Risk Area Identification Model

Combined with the actual situation and background of the risk level assessment of the functional area of the bus stop, this study divides the functional area by rasterization and uses the gray clustering evaluation method to construct the risk area identification model.

4.1. Evaluation Object. Carry out rasterization processing on the bus stop functional area, and take each grid as the evaluation object. Taking the lower left corner of the bus stop as the origin of the coordinates, the direction of the traffic flow is the X-axis direction, and the side away from the bus stop is the Y-axis direction to establish a Cartesian two-dimensional coordinate system. The X-axis direction divides the bus stop functional areas at intervals of 10 meters; the Y-axis direction uses the lane mark as the dividing line. After processing, the evaluation object number is shown in Figure 8.

4.2. Evaluation Indicator. A scientific and objective evaluation indicator system is the key to constructing a risk area identification model. According to the traffic characteristics, the evaluation indicator system constructed in this paper mainly includes three aspects: conflict rate, average severity index of conflict, and potential conflict risk index.
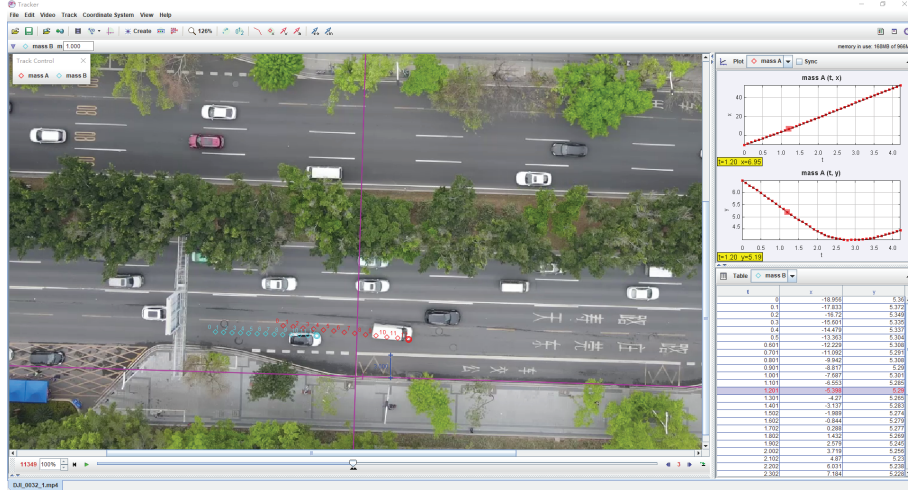
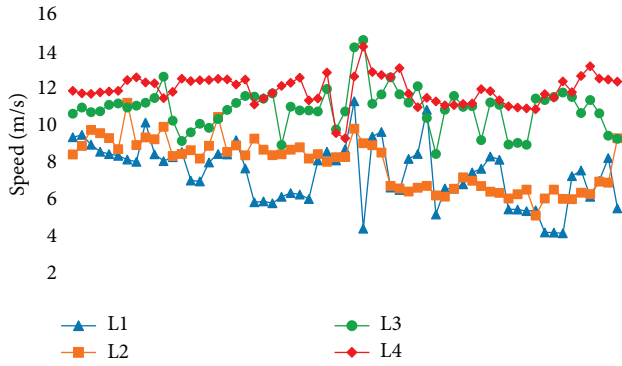FIGURE 5: Schematic diagram of extracting lane-change conflicts.

FIGURE 6: Speed distribution of lanes.

TABLE 1: Speed distribution characteristics of lanes.

	Lane 1	Lane 2	Lane 3	Lane 4
Average speed (m/s)	7.438	8.755	10.884	12.594
Standard deviation (m/s)	1.614	1.359	1.129	0.809

4.2.1. Conflict Rate. The conflict rate k_1 can be defined as the ratio between the number of conflicts in a single evaluation object and the total number of conflicts in the entire bus stop functional area. The calculation formula of the conflict rate k_1 is shown in the following equation:

$$k_1 = \frac{TC_i}{\sum_{i=1}^{n} TC_i}. \tag{3}$$

4.2.2. Average Severity Index of Conflicts. The severity index (SI) represents the severity of traffic conflicts in the grid [44]. The calculation formula for converting TTC to SI is shown in the following equation:

$$SI = \exp\left(-\frac{TTC^2}{2PRT^2}\right). \tag{4}$$

Here, PRT represents the driver's braking response time, usually 2.5 seconds. SI is a dimensionless index, between 0 and 1; the larger the value, the more serious the conflict. In a certain grid, the arithmetic mean of the severity index is recorded as the average severity index of conflict k_2, and the calculation formula can be sorted into the following equation:

$$k_2 = \frac{\sum_{i=1}^{n} SI_i}{n}. \tag{5}$$

4.2.3. Potential Conflict Risk Index. The potential conflict risk index k_3 is the potential conflict risk at the location of a certain area, which can be defined as the average value of the conflict rate in adjacent areas. The calculation formula of k_3 is shown in the following equation:

$$k_3 = \frac{\sum_{q=1}^{Q} TC_q}{\sum_{i=1}^{n} TC_i} * \frac{1}{Q}. \tag{6}$$

4.3. Risk Level and Whitening Weight Function. In terms of the number of security levels, they are generally divided into two to ten levels [13, 14, 45, 46]. According to the actual situation, the risk level is divided into four levels: safe, relatively safe, critically safe, and unsafe. The cumulative frequency curve is typically used for determining safe speed limit [47]. This paper uses the cumulative frequency curve to determine the whitening value. First, it calculates the cumulative percentage frequency of each index, draws the cumulative percentage frequency curve graph, and then obtains the corresponding abscissa values at 15%, 40%, 60%, and 85%, that is, the whitening values (A_1), (A_2), (A_3), (A_4) of each gray category in the corresponding indicators. The cumulative frequency curve is shown in Figure 9.

In 2014, Gao et al. proposed a center-point mixed whitenization weight function, which reduces the requirement of clustering index and has a broad application prospect [48, 49]. The function formula is shown in equations (7)–(10), and the function image is shown in Figure 10.
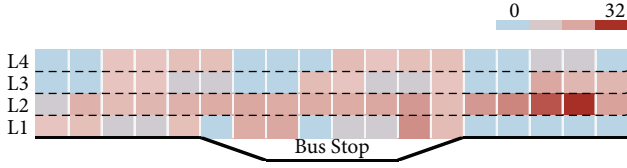
FIGURE 7: Lane-changing location heat map.

$$f_1(x) = \begin{cases} 0, & x > A_2, \\ \dfrac{A_2 - x}{A_2 - A_1}, & x \in [A_1, A_2], \\ 1, & x < A_1, \end{cases} \tag{7}$$

$$f_2(x) = \begin{cases} 0, & x \notin [A_1, A_3], \\ \dfrac{x - A_1}{A_2 - A_1}, & x \in [A_1, A_2], \\ \dfrac{A_3 - x}{A_3 - A_2}, & x \in [A_2, A_3], \end{cases} \tag{8}$$

$$f_3(x) = \begin{cases} 0, & x \notin [A_2, A_4], \\ \dfrac{x - A_2}{A_3 - A_2}, & x \in [A_2, A_3], \\ \dfrac{A_4 - x}{A_4 - A_3}, & x \in [A_3, A_4], \end{cases} \tag{9}$$

$$f_4(x) = \begin{cases} 0, & x < A_3, \\ \dfrac{x - A_3}{A_4 - A_3}, & x \in [A_3, A_4], \\ 1, & x > A_4. \end{cases} \tag{10}$$

4.4. Index Weight.

Entropy is a measure of the degree of disorder in the system. The more information there is, the less uncertainty and less entropy there is. The greater the dispersion degree of the index, the greater the influence of the index on the comprehensive evaluation [50]. If a certain index value of all evaluation objects is equal, the index has no influence in the comprehensive evaluation, and the weight is zero. According to the definition of entropy, the weight θ_j of index j can be calculated by the following equations:

$$E_j = -\frac{1}{\ln(n)} \sum_{i=1}^{n} \frac{X_{ij}}{\sum_{i=1}^{n} X_{ij}} \ln\left(\frac{X_{ij}}{\sum_{i=1}^{n} X_{ij}}\right), \tag{11}$$

$$\theta_j = \frac{1 - E_j}{m - \sum_{j=1}^{m} E_j}. \tag{12}$$

Here, X_{ij} is the normalized data of the i-th object under the j-th index; when $(X_{ij}/\sum_{i=1}^{n} X_{ij}) = 0$, let $\ln(X_{ij}/\sum_{i=1}^{n} X_{ij}) = 0$.

The limitation of the entropy method is that it only depends on the degree of fluctuation of the data; that is, the weight is obtained from the objective amount of information, without considering the actual meaning of the data, so the results obtained may not conform to the general rule. By combining weighting with the subjective weight η_j, the indicator weight can be more in line with the actual situation. The combination weighting calculation formula of index j is shown in the following equation:

$$w_j = \vartheta\theta_j + (1 - \vartheta)\eta_j. \tag{13}$$

Here, ϑ is the ratio between the weight of the entropy weighting method and the weight of the combination.

4.5. Gray Clustering Coefficient Calculation.

Let σ_i^k be the clustering coefficient of the i-th object for the k-th gray class; then, σ_i^k can be calculated by the equation:

$$\sigma_i^k = \sum_{j=1}^{n} f_{jk}(d_{ij}) \times w_j. \tag{14}$$

4.6. Determining Clustering Results.

People usually classify the decision objects only according to the maximum value of gray clustering coefficients. Although the results obtained are reasonable, they are sometimes biased, especially when the maximum value of clustering coefficients is not significantly different from the rest of the coefficients [51]. To avoid this problem, this paper uses the two stages of the decision model with gray synthetic measure to analyze the clustering coefficients. For object i that needs to be determined, if the difference between the first largest coefficient and the second largest coefficient is greater than 0.125, the clustering result is considered clear, which can be done by $\max_{1 \leq k \leq s}\{\delta_i^k\} = \delta_i^{k^*}$ to determine that object i belongs to the gray category k^*. Otherwise, calculate the comprehensive weighted decision vector φ_k. The calculation formula of φ_k is shown in the following equations:

$$\varphi_1 = \frac{2}{s(s+1)}, \quad s, s-1, s-2, \dots, 1, \tag{15}$$

$$\varphi_2 = \frac{1}{(s(s+1)/2) + (s-2)}, \quad s-1, s, s-1, \dots, 2, \tag{16}$$

$$\varphi_k = \frac{1}{(s(s+1)/2) + ((k-1)s - (k(k-1)/2))}, \\ s-k+1, s-k+2, \dots, k, \tag{17}$$

$$\varphi_{s-1} = \frac{2}{(s(s+1)/2) + (s-2)}, \quad 2, 3, \dots, s, s-1, \tag{18}$$

$$\varphi_s = \frac{2}{s(s+1)}, \quad 1, 2, \dots, s-1, s. \tag{19}$$

Finally, use $w_i^k = \varphi_k \delta_i^T$ to calculate the gray comprehensive measure decision coefficient of object i with respect
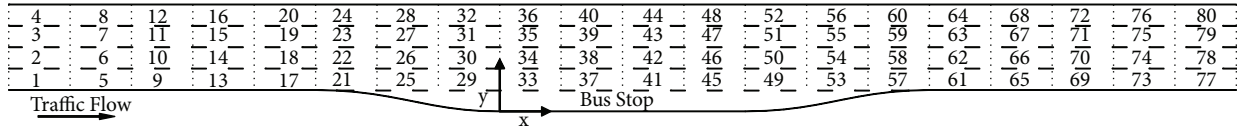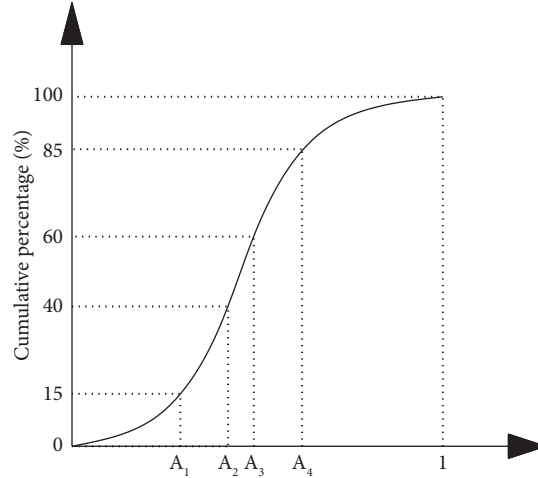
FIGURE 8: Schematic of the evaluation object.

FIGURE 9: Cumulative frequency curve.

to gray class k. According to $\max_{1 \leq k \leq s}\{w_i^k\} = w_i^{k*}$, the judgment that object i belongs to the gray category k^* is completed.

5. Application of the Risk Area Identification Model

5.1. Risk Level Calculation. In this paper, the research object is a bus bay stop located on a four-lane expressway, which is divided into 80 grid samples. Take the conflict rate, severity index of conflict, and potential conflict risk index as the evaluation indicators. Denote the sample evaluation matrix as U; then, the sample matrix is as follows:

$$U = \begin{bmatrix} 0.0000 & 0.0000 & 0.0298 \\ 0.0500 & 0.7025 & 0.0179 \\ 0.0000 & 0.0000 & 0.0536 \\ \cdots & \cdots & \cdots \\ 0.0000 & 0.0000 & 0.3274 \end{bmatrix}. \quad (20)$$

The whitening values of the evaluation index obtained by the cumulative frequency curve method are shown in Table 2.

The clustering coefficient of each grid for each gray category is obtained through the risk area identification

model, and then the risk level of each grid is judged. The gray classification results of each grid are shown in Table 3. Among them, the grids with significant difference coefficients that do not meet the requirements need to be judged in the second stage, and the classification results of the second stage are shown in Table 4.

5.2. Analysis of the Risk Area in Bus Bay Stops. Figure 11 shows the grid risk level results within the bus stop, and the risk area distribution obtained by linear interpolation is shown in Figure 12.

It can be seen that the traffic conflicts in the functional area of the bus stop are mainly concentrated in the middle and lower reaches of the stop. Therefore, it can be concluded that the impact of bus exiting on traffic safety is higher than entering the station. The risk of traffic conflicts is relatively high in the area where the transition section of the bus stop meets the mainline road. The main reason is that, during the exit process, there is a large difference between the speed of the bus and the speed of the vehicles on the main line. When encountering a bus exiting the stop, the vehicles on the main line will take actions such as slowing down or changing lanes to avoid the danger. From a horizontal point of view, the risk of traffic conflicts on lane 2 and lane 3 is relatively high; the traffic conflicts on lane 4 are widely distributed; and the number of conflicts on lane 1 is relatively small.
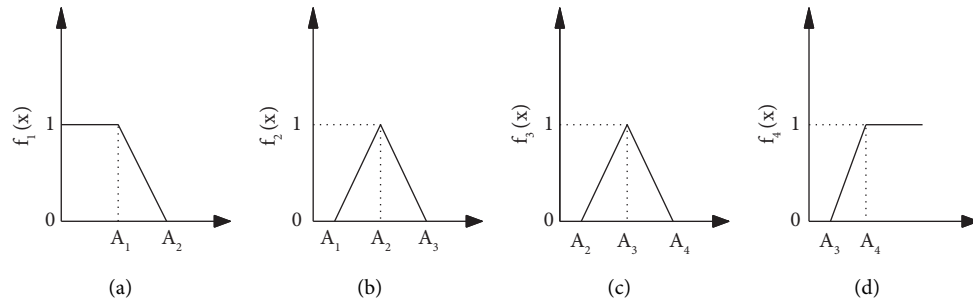
FIGURE 10: Schematic diagram of whitenization weight function.

TABLE 2: Whiting values of each evaluation index.

Whiting value	k_1	k_2	k_3
A_1	0.0296	0.2495	0.0666
A_2	0.0915	0.6207	0.2885
A_3	0.1722	0.7190	0.3477
A_4	0.3263	0.8515	0.4833

TABLE 3: Results of clustering coefficient and its classification.

Object number	Clustering coefficient				Significant coefficient	Whether to enter the second stage of decision-making	Classification
	δ_i^1	δ_i^2	δ_i^3	δ_i^4			
1	1.0000	0.0000	0.0000	0.0000	1.0000	No	1
2	0.4061	0.1664	0.4275	0.0000	0.0214	Yes	To be determined
3	1.0000	0.0000	0.0000	0.0000	1.0000	No	1
...	...	...	...	...	...	...	...
33	0.0000	0.6588	0.3412	0.0000	0.3177	No	2
34	0.0000	0.0670	0.8484	0.0846	0.7639	No	3
35	0.0000	0.0000	0.3465	0.6535	0.3071	No	4
36	0.1632	0.0802	0.3798	0.3767	0.0031	Yes	To be determined
37	0.0000	0.2178	0.3731	0.4090	0.0359	Yes	To be determined
38	0.0000	0.0000	0.2275	0.7725	0.5450	No	4
39	0.0000	0.3949	0.3863	0.2188	0.0086	Yes	To be determined
...	...	...	...	...	...	...	...
80	0.7572	0.0833	0.1595	0.0000	0.5977	No	1

TABLE 4: Results of the comprehensive clustering coefficient and its classification.

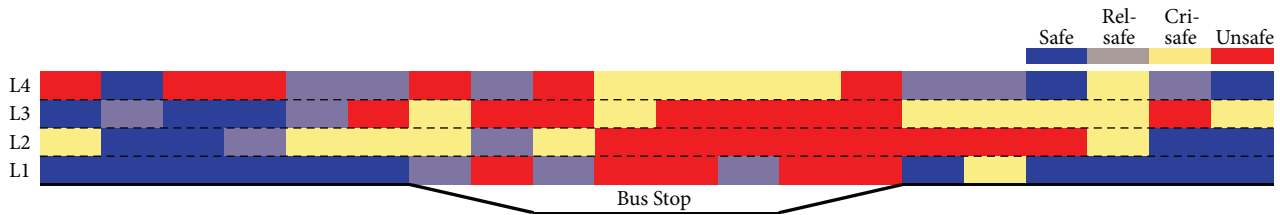| Object number	Comprehensive clustering coefficient				Classification
	w_i^1	w_i^2	w_i^3	w_i^4	
2	0.2979	0.2639	0.2518	0.2021	1
4	0.2379	0.2139	0.2162	0.2621	4
16	0.2373	0.2143	0.2166	0.2627	4
23	0.2132	0.2338	0.2677	0.2868	4
36	0.2030	0.2253	0.2680	0.2970	4
...	...	...	...	...	...
79	0.2655	0.2573	0.2596	0.2345	1

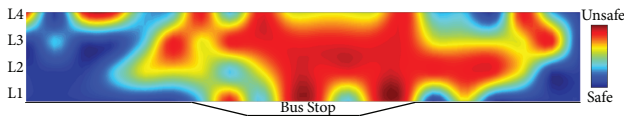Figure 11: Results of internal risk assessment of bus stops.

Figure 12: Distribution of risk region within bus stops.

6. Conclusions

When studying the safety performance of bus stops, most scholars have evaluated it as a whole [16], thus ignoring the differences in risk levels of different lanes within the functional area of the bus stop. In this study, we demonstrate that the risk levels in different areas within the bus stop functional area are not the same through the traffic conflict technology. These findings can help us to better understand the risk distribution in bus stop functional areas and provide valuable suggestions for intervention strategies to improve road safety. A bus stop is analyzed as an example through the proposed risk area identification model, and the following conclusions are drawn:

(1) The risk area of a bus bay stop is mainly concentrated in the middle and lower reaches of the functional area. The impact of bus exiting on traffic safety is higher than entering the station. The risk of traffic conflicts near the transition section of the bus stop is higher.

(2) The conflicts on lane 1 close to the bus stop are relatively concentrated, and the severity of conflicts is low. There are many dangerous areas on lane 2 and lane 3, and the traffic conflicts are the most serious. The dangerous areas of lane 4 are widely distributed, and the severity of the conflict is relatively high.

(3) The distribution of the risk area and the lane-changing point has certain similar characteristics. There are many lane-changing points on lane 2, and the corresponding traffic conflict risk is also higher. In the future, by prohibiting lane changes of vehicles near bus stops, it may be possible to reduce the risk of traffic conflicts and improve safety performance.

Data Availability

All the data (characteristics of bus stops and traffic conditions of bus stops) used to support the findings of this study are included within the article.

Conflicts of Interest

The authors declare that there are no conflicts of interest regarding the publication of this paper.

Acknowledgments

References

[1] X. Zhang, S. Hao, R. WenGe, and D. Cooper, "Intelligent transportation systems for smart cities: a progress review," *Science China Information Sciences*, vol. 55, pp. 2908–2914, 2012.

[2] Y. Liu and Y. Nie, "A credit-based congestion management scheme in general two-mode networks with multiclass users," *Networks and Spatial Economics*, vol. 17, no. 3, pp. 681–711, 2017.

[3] Y. Li, Y. Liu, and J. Xie, "A path-based equilibrium model for ridesharing matching," *Transportation Research Part B: Methodological*, vol. 138, pp. 373–405, 2020.

[4] X. Yang, W. Jin, H. Jiang, Q. Xie, W. Shen, and W. Han, "Car ownership policies in China: preferences of residents and influence on the choice of electric cars," *Transport Policy*, vol. 58, pp. 62–71, 2017.

[5] X. Qu and S. Wang, "Communications in transportation research: vision and scope," *Communications in Transportation Research*, vol. 1, Article ID 100001, 2021.

[6] J. Wu, B. Kulcsár, Selpi, and X. Qu, "A modular, adaptive, and autonomous transit system (MAATS): an in-motion transfer strategy and performance evaluation in urban grid transit networks," *Transportation Research Part A: Policy and Practice*, vol. 151, pp. 81–98, 2021.

[7] Y. Bie, X. Xiong, Y. Yan, and X. Qu, "Dynamic headway control for high-frequency bus line based on speed guidance and intersection signal adjustment," *Computer-Aided Civil and Infrastructure Engineering*, vol. 35, no. 1, pp. 4–25, 2020.

[8] Y. Bie, J. Ji, X. Wang, and X. Qu, "Optimization of electric bus scheduling considering stochastic volatilities in trip travel time and energy consumption," *Computer-Aided Civil and Infrastructure Engineering*, vol. 36, no. 12, pp. 1530–1548, 2021.

[9] L. Zhang, S. Wang, and X. Qu, "Optimal electric bus fleet scheduling considering battery degradation and non-linear charging profile," *Transportation Research Part E:*

Transportation and Logistics Review, vol. 154, Article ID 102445, 2021.

[10] X. Zhang, Q. Zhang, T. Sun, Y. Zou, and H. Chen, "Evaluation of urban public transport priority performance based on the improved TOPSIS method: a case study of Wuhan," *Sustainable Cities and Society*, vol. 43, pp. 357–365, 2018.

[11] I. Peled, K. Lee, Y. Jiang, J. Dauwels, and F. C. Pereira, "On the quality requirements of demand prediction for dynamic public transport," *Communications in Transportation Research*, vol. 1, Article ID 100008, 2021.

[12] Q. Meng and X. Qu, "Bus dwell time estimation at bus bays: a probabilistic approach," *Transportation Research Part C: Emerging Technologies*, vol. 36, pp. 61–71, 2013.

[13] Z. Ye, C. Wang, Y. Yu, X. Shi, and W. Wang, "Modeling level-of-safety for bus stops in China," *Traffic Injury Prevention*, vol. 17, no. 6, pp. 656–661, 2016.

[14] D. Chimba, T. Sando, and V. Kwigizile, "Effect of bus size and operation to crash occurrences," *Accident Analysis & Prevention*, vol. 42, no. 6, pp. 2063–2067, 2010.

[15] M. Amadori and T. Bonino, "A methodology to define the level of safety of public transport bus stops, based on the concept of risk," *Procedia-Social and Behavioral Sciences*, vol. 48, pp. 653–662, 2012.

[16] M. F. Cheranchery, K. Bhattacharyya, M. Salih, and B. Maitra, "A proactive approach to assess safety level of urban bus stops," *International Journal of Injury Control and Safety Promotion*, vol. 26, no. 3, pp. 260–270, 2019.

[17] L. Truong and S. Somenahalli, "Using GIS to identify pedestrian-vehicle crash hot spots and unsafe bus stops," *Journal of Public Transportation*, vol. 14, no. 1, pp. 99–114, 2011.

[18] A. Charly and T. V. Mathew, "Estimation of traffic conflicts using precise lateral position and width of vehicles for safety assessment," *Accident Analysis & Prevention*, vol. 132, Article ID 105264, 2019.

[19] K. Xie, C. Li, K. Ozbay et al., "Development of a comprehensive framework for video-based safety assessment," in *Proceedings of the IEEE 19th International Conference on Intelligent Transportation Systems (ITSC)*, pp. 2638–2643, Rio de Janeiro, Brazil, November 2016.

[20] K. El-Basyouny and T. Sayed, "Safety performance functions using traffic conflicts," *Safety Science*, vol. 51, no. 1, pp. 160–164, 2013.

[21] A. P. Tarko, "Estimating the expected number of crashes with traffic conflicts and the Lomax distribution-a theoretical and numerical exploration," *Accident Analysis & Prevention*, vol. 113, pp. 63–73, 2018.

[22] Q. Meng and X. Qu, "Estimation of rear-end vehicle crash frequencies in urban road tunnels," *Accident Analysis & Prevention*, vol. 48, pp. 254–263, 2012.

[23] Y. Kuang, Y. Yu, and X. Qu, "Novel crash surrogate measure for freeways," *ASCE Journal of Transportation Engineering Part A: Systems*, vol. 146, Article ID 4020085, 2020.

[24] Y. Kuang, X. Qu, and S. Wang, "A tree-structured crash surrogate measure for freeways," *Accident Analysis & Prevention*, vol. 77, pp. 137–148, 2015.

[25] Z. Zheng, "Reasons, challenges, and some tools for doing reproducible transportation research," *Communications in Transportation Research*, vol. 1, Article ID 100004, 2021.

[26] Y. Wang, Z. Li, Z. Ye, and Y. Zhang, "Nighttime safety evaluation for signalized intersections at the signal cycle level based on rear-end conflict models considering lighting and traffic conditions," *Traffic Injury Prevention*, vol. 21, no. 1, pp. 87–92, 2020.

[27] Y. Guo, T. Sayed, and M. Essa, "Real-time conflict-based bayesian tobit models for safety evaluation of signalized intersections," *Accident Analysis & Prevention*, vol. 144, Article ID 105660, 2020.

[28] M. Ghanim, M. Kharbeche, J. Hannun, J. Hannun, and K. Shamiyeh, "Safety and operational performance of signalized roundabouts: a case study in doha," *Procedia Computer Science*, vol. 170, pp. 427–433, 2020.

[29] X. Shi, Z. Wang, X. Li, and M. Pei, "The effect of ride experience on changing opinions toward autonomous vehicle safety," *Communications in Transportation Research*, vol. 1, Article ID 100003, 2021.

[30] Y. Ma, H. Meng, S. Chen, J. Zhao, and P. E. Shen, "Predicting traffic conflicts for expressway diverging areas using vehicle trajectory data," *Journal of Transportation Engineering*, vol. 146, Article ID 4020003, 2020.

[31] H. Ge and Y. Yang, "Research on calculation of warning zone length of freeway based on micro-simulation model," *IEEE Access*, vol. 8, pp. 76532–76540, 2020.

[32] B. Su and N. Xie, "Research on safety evaluation of civil aircraft based on the grey clustering model," *Grey Systems: Theory and Application*, vol. 8, no. 1, pp. 110–120, 2018.

[33] D. Luo, L. Ye, Y. Zhai, H. Zhu, and Q. Qian, "Hazard assessment of drought disaster using a grey projection incidence model for the heterogeneous panel data," *Grey Systems: Theory and Application*, vol. 8, no. 4, pp. 509–526, 2018.

[34] H. Wu and J. Wang, "Waterlogging hazard assessment of deep foundation pit projects based on fowa operator and gray clustering," *Journal of Nonlinear and Convex Analysis*, vol. 21, pp. 1839–1849, 2020.

[35] Y. Tian, X. Sun, L. Chen, and L. Huang, "Risk assessment of nautical navigational environment based on grey fixed weight cluster," *Promet-Traffic & Transportation*, vol. 29, no. 3, pp. 331–342, 2017.

[36] N. Zhou, S. Wang, J. Xi, and Y. Chaoyang, "Grey synthetic degree of incidence entropy and its application in traffic accidents analysis," *Journal of Grey System*, vol. 22, pp. 257–264, 2010.

[37] W. Yi, S. Wang, Y. Jin, and J. Cao, "Integrated computer vision algorithms and drone scheduling," *Communications in Transportation Research*, vol. 1, Article ID 100002, 2021.

[38] N. Nadimi, D. R. Ragland, and A. Mohammadian Amiri, "An evaluation of time-to-collision as a surrogate safety measure and a proposal of a new method for its application in safety analysis," *Transportation Letters*, vol. 12, no. 7, pp. 491–500, 2020.

[39] X. Qu, Y. Yu, M. Zhou, C.-T. Lin, and X. Wang, "Jointly dampening traffic oscillations and improving energy consumption with electric, connected and automated vehicles: a reinforcement learning based approach," *Applied Energy*, vol. 257, Article ID 114030, 2020.

[40] Y. Xu, Y. Zheng, and Y. Yang, "On the movement simulations of electric vehicles: a behavioral model-based approach," *Applied Energy*, vol. 283, Article ID 116356, 2021.

[41] L. N. Peesapati, M. P. Hunter, and M. O. Rodgers, "Evaluation of postencroachment time as surrogate for opposing left-turn crashes," *Transportation Research Record: Journal of the Transportation Research Board*, vol. 2386, no. 1, pp. 42–51, 2013.

[42] A. Laureshyn, A. Svensson, and C. Hydén, "Evaluation of traffic safety, based on micro-level behavioural data: theoretical framework and first implementation," *Accident Analysis & Prevention*, vol. 42, no. 6, pp. 1637–1646, 2010.

[43] G. Lu, M. Liu, Y. Wang, and G. Yu, "Quantifying the severity of traffic conflict by assuming moving elements as rectangles

at intersection," *Procedia-Social and Behavioral Sciences*, vol. 43, pp. 255–264, 2012.

[44] J. Autey, T. Sayed, and M. H. Zaki, "Safety evaluation of right-turn smart channels using automated traffic conflict analysis," *Accident Analysis & Prevention*, vol. 45, pp. 120–130, 2012.

[45] X. Cai, C. Lei, B. Peng, X. Tang, and Z. Gao, "Road traffic safety risk estimation method based on vehicle onboard diagnostic data," *Journal of Advanced Transportation*, vol. 2020, Article ID 3024101, 13 pages, 2020.

[46] M. Ahmadpur and I. Gokasar, "Spatial analysis and evaluation of road traffic safety performance indexes across the provinces of Turkey from 2015 to 2019," *International Journal of Injury Control and Safety Promotion*, vol. 28, no. 3, pp. 309–324, 2021.

[47] J. Xu, W. Lin, X. Wang, and Y.-M. Shao, "Acceleration and deceleration calibration of operating speed prediction models for two-lane mountain highways," *Journal of Transportation Engineering, Part A: Systems*, vol. 143, Article ID 04017024, 2017.

[48] K. Gao, L. Sun, Y. Yang, F. Meng, and X. Qu, "Cumulative prospect theory coupled with multi-attribute decision making for modeling travel behavior," *Transportation Research Part A: Policy and Practice*, vol. 148, pp. 1–21, 2021.

[49] S. Liu, L. Tao, N. Xie, and Y. Yang, "On the new model system and framework of grey system theory," in *Proceedings of the IEEE International Conference on Grey Systems and Intelligent Services (GSIS)*, pp. 1–11, Leicester, UK, August 2015.

[50] Y. Shao, X. Han, H. Wu, and C. Claudel, "Evaluating signalization and channelization selections at intersections based on an entropy method," *Entropy*, vol. 21, Article ID 21080808, 2019.

[51] S. Liu, Y. Yang, and Z. Fang, "A new decision model to solve the clustering dilemma," in *Proceedings of the IEEE International Conference on Systems, Man, and Cybernetics (SMC)*, pp. 000115–000121, Budapest, Hungary, October 2016.